Available online at www.sciencedirect.com
ScienceDirect
Journal of Electroanalytical Chemistry 613 (2008) 16–22
Journal of Electroanalytical Chemistry
www.elsevier.com/locate/jelechem

Oxide/hydroxide films on tin. II: Characterization of the anodic growth in alkaline solutions

V. Brunetti, M. López Teijelo *

INFIQC – Departamento de Fisicoquímica, Facultad de Ciencias Químicas, Universidad Nacional de Córdoba, Haya de la Torre y Medina Allende, 5000 Córdoba, Argentina

Received 8 May 2007; received in revised form 26 September 2007; accepted 1 October 2007
Available online 6 October 2007

Abstract

The anodic growth of oxide/hydroxide films formed on tin in borate solutions (pH 8.9) has been studied. At potentials more positive than −0.2 V (SHE), oxide film growth occurs by an activation-controlled ionic condition under the influence of a high electric field across the film according to an exponential law as on valve metals. Optical properties of the anodic oxide films have been obtained by ''in situ'' ellipsometry. Tin oxide/hydroxide films are practically transparent and highly hydrated. Electrical properties of tin oxide layers have been obtained by electrochemical impedance spectroscopy. Impedance spectra are explained in terms of a simple physical model assuming that oxide layer behaves as an inhomogeneous single-layer film.

Keywords: Tin oxide; Oxide/hydroxide layers; High-field growth; Ellipsometry; Electrochemical impedance spectroscopy

1. Introduction

The electrochemical behaviour of tin oxide formation in aqueous media has been extensively studied mainly in alkaline solutions. The kinetics of the oxide/hydroxide film formation has been the subject of many studies and is reviewed briefly in Part I of this series [1]. Different mechanisms have been proposed for the active to passive transition as well as the anodic oxide film growth, although the understanding of the kinetics of the film formation is not fully understood. Kapusta et al. [2–4] had reported that under potentiostatic or galvanostatic conditions, passivation of tin shows behaviour similar to that observed on ''valve'' metals. Ammar et al. [5,6] has found that in acid, neutral and alkaline electrolytes the kinetics of oxidation on tin presents also the characteristics of valve metals. On the contrary, Metikos et al. [7] claimed that under potentiodynamic conditions, tin oxide formation is controlled by ohmic resistance although under galvanostatic conditions, they reported that anodic film growth occurs by activation-controlled ion conduction under the influence of a high electric field.

In this paper, we report on the results obtained by applying triangular potential sweeps as well as in situ ellipsometric and electrochemical impedance spectroscopy (EIS) measurements during the anodic growth of tin oxide/hydroxide films on tin in alkaline borate solutions at potentials more positive than −0.2 V (SHE).

2. Experimental

The working electrode consisted of a polycrystalline tin rod (Koch-Light, 99.999% purity) of 8 mm diameter mounted in a Teflon holder which exposes a circular area of 0.50 cm^2. Before the experiments the electrode surface was abraded with emery paper, then polished mechanically with diamond paste (9 and 3 μm) dispersed with etileneglycol on a nylon cloth (Buehler) and alumina (1, 0.3 and 0.05 μm) on a polishing cloth (Microcloth, Buehler). Then

* Corresponding author. Tel.: +54 351 4334169; fax: +54 351 4334188.
E-mail address: mlopez@mail.fcq.unc.edu.ar (M. López Teijelo).

0022-0728/$ - see front matter © 2007 Elsevier B.V. All rights reserved.
doi:10.1016/j.jelechem.2007.10.001

the electrode was cleaned repeatedly with purified water, immersed in the solution and cathodized at −1.29 V for 10 min before the experiments.

The electrochemical measurements were performed in a three-compartment electrolysis cell using a gold sheet as counterelectrode and a $Hg/Hg_2SO_4/Na_2SO_4$ (1 M) as reference electrode. Nevertheless, all potentials are referred to the standard hydrogen electrode (SHE).

Solutions of $Na_2B_4O_7$ (pH 8.9) were prepared from AR chemicals and purified water (Milli Ro-Milli Q system). Measurements were performed at 25 °C under nitrogen gas saturation.

Electrochemical measurements were done by applying single or repetitive triangular potential sweeps between preset lower ($E_{s,c}$) and upper ($E_{s,a}$) switching potentials at different scan rates (v). Several potential time routines were used, changing the holding time and the values of $E_{s,c}$ and $E_{s,a}$. These routines are specified in each voltammogram. EIS measurements were carried out at the open circuit potential employing an Impedance Spectrum Analyzer Zahner IM5D. The amplitude of the perturbation signal was 10 mV and the frequency range was 0.1 Hz–10 kHz.

Ellipsometric data were obtained by using a three-compartment cell made of Pyrex glass. The working electrode was mounted in a Teflon holder and placed horizontally in the cell compartment provided with two plane glass windows adequate for optical measurements. The electrolysis cell was mounted in a Rudolph Research rotating-analyser automatic ellipsometer (vertical type, 2000 FT model) equipped with a 75 W tungsten lamp as light source and a filter (546.1 nm). The light reflected by the electrode surface passed through a rotating analyser to a photomultiplier tube (PMT) for detection. The sinusoidal output of the PMT was digitised by a HP 216 microcomputer and the values of ψ and Δ were calculated by the computer from the three Fourier coefficients of the PMT signal. The PMT signal was averaged twice and data were collected in continuous mode. The time interval between measurements was *ca.* 1 s. All measurements were made at an incidence angle of 70.00°. The experimental data were fitted employing a model for a single isotropic film, using the Simplex method [8] to minimize the function $G = \Sigma(\Delta^{exp} - \Delta^{th})^2 + (\Psi^{exp} - \Psi^{th})^2$.

3. Results and discussion

3.1. Electrochemical behaviour

In Part I [1] we have described the j/E potentiodynamic response of polycrystalline tin electrodes in borate solutions (pH 8.9) obtained by applying triangular potential sweeps (Fig. 1). After anodic current peaks I and II obtained in the positive scan, which are associated with the stepwise oxidation of Sn to Sn (IV) species leading to the formation of the tin oxide/hydroxide films producing primary tin passivation, a nearly stationary current plateau (III) is obtained up to *ca.* 1.8 V where oxygen evolution

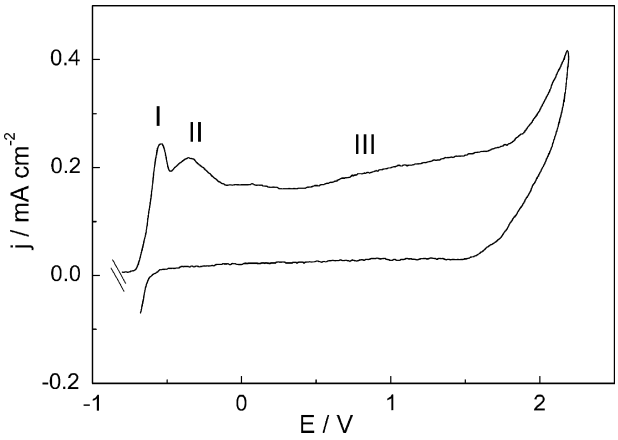

Fig. 1. Potentiodynamic j/E profile for Sn in borate solutions (pH 8.9). Sweep rate: 0.050 V s^{-1}.

takes place. This broad potential range where a nearly steady-state current is seen corresponds to the film growth in the passive state [2].

The kinetic analysis during the electroformation and electroreduction of tin oxide/hydroxide films in the −1.5 V to −0.2 V potential range indicated that both processes are controlled by ohmic resistance [1]. The passivating layer grows and spreads across the surface until only small pores in the layer remain and the overall rate is controlled by the resistance in the pores. Then, a continuous film grows at potentials more positive than −0.2 V.

In order to ascertain the kinetics of growth of the anodic oxide/hydroxide film at potentials more positive then −0.2 V, some combined potential/time routines as those employed for obtaining the separation of the different anodic peaks in the potentiodynamic response of iron in bicarbonate solutions [9], were applied. For this purpose, potential holdings in the potential range of peak I ($-0.63\ V \leqslant E_\tau \leqslant -0.55\ V$) during the positive potential scan were applied for different holding times (Fig. 2). For low E_τ values or short holding times, current density does not drop to low values and the j/E profile obtained after

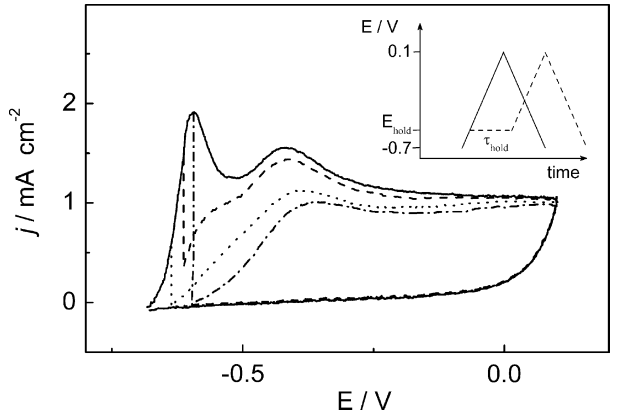

Fig. 2. j/E response obtained applying the potential-time routine indicated in the inset, changing t and E_t values.

the potential holding exhibits the two anodic current contributions in the potential region of peaks I and II before the steady-state current plateau. The different contributions are dependent on E_τ as well as the holding time. In contrast, for $E_\tau = -0.55$ V and a holding time allowing the anodic current drop almost to zero, peaks I and II are practically absent and the positive scan exhibits only the stationary current plateau corresponding to the anodic growth. In the negative potential scan, the current drops rapidly to very low values and film growth stops.

The potentiodynamic j/E response described above, that is a current increase reaching a steady-state current value in a broad potential range, is characteristic of anodic oxide growth by an ionic-conduction mechanism under the influence of a high electric field across the film as in typical "valve" metals like Ti, Zr, W, etc. [10,11].

As an additional proof of the validity of the high-field model for the oxide growth at potentials more positive than *ca.* −0.2 V, voltammograms run by applying repetitive triangular potential sweeps with a progressive increase of the upper switching potential ($E_{s,a}$) value, were obtained (Fig. 3). During the first positive scan the anodic current peaks I and II as well as the steady-state current for oxide growth, are obtained. In the negative scan the current drops to a very low value and at potentials more negative than *ca.* −0.7 V the cathodic peak corresponding to the overall oxide film electroreduction is seen. From the second cycle onwards, the anodic current increases at potentials close to the $E_{s,a}$ value of the previous cycle and reaches the same value corresponding to the steady-state value. The absence of curve-crossing between successive cycles indicates that there is no chemical dissolution of the film, at least in the time of the experiment. The j/E potentiodynamic response described above is typical for the growth of an oxide layer on "valve" metals by a high-field mechanism [10,12]. In this case, when anodically polarized "valve" metals oxidation follows the "high-field" law [10,12]:

$$j = A\exp(\beta \overline{E}) \tag{1}$$

where j is the ionic current density for anodic oxide growth, $\overline{E}$ is the electric field within the oxide, and A and β are temperature-dependent characteristic parameters of the oxide. For the potentiodynamic oxide growth, provided that the potential drop at the interfaces is negligible and in the absence of space charge effects, the following expression is obtained [12] for the steady-state current density (j_{ss}):

$$j_{ss}\ln\left(\frac{j_{ss}}{A}\right) = \frac{nF\delta_{ox}}{M}\beta v \tag{2}$$

where δ_{ox} is the oxide film density, M is the molecular weight and n the number of electrons exchanged in the oxide formation reaction. According to Eq. (2), j_{ss} increases almost linearly with scan rate, v, as $\ln(j_{ss}/A)$ is a slowly increasing function with scan rate. The usual practice for obtaining the value of the parameters A and β, is plotting $\ln j_{ss}$ vs (v/j_{ss}). Fig. 4 shows the dependence obtained, from which the values $A = (2.7 \pm 2) \times 10^{-8}$ A cm^{-2} and $\beta = (1.2 \pm 0.1) \times 10^{-6}$ V^{-1} cm, are obtained. These figures are comparable to those obtained for the growth of other oxides [11].

3.2. Ellipsometric characterization

In order to obtain the optical properties of the tin oxide films as well the dependence of oxide thickness with growth potential, the "in situ" ellipsometric response during the potentiodynamic growth of oxide/hydroxide films on tin, was obtained. Fig. 5 shows the evolution of the ellipsometric angles Ψ and Δ with time during the potentiodynamic anodization at 0.050 V s^{-1} of polished tin electrodes in alkaline borate solutions. Four different regions with distinct optical response, mainly seen as breaks in the Δ/t dependence can be observed:

Region 1: from 0 up to *ca.* 8 s (covering the −0.75 V to −0.2 V potential range), which corresponds to the stepwise electroformation of the $Sn(OH)_2$/SnO film and the subsequent oxidation to $Sn(OH)_4$ (anodic current peaks I and II).

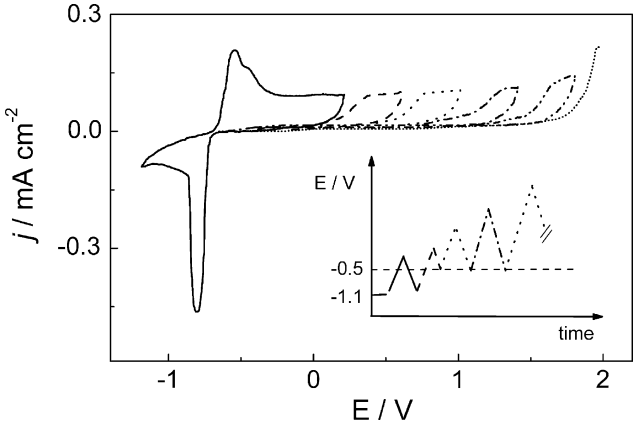

Fig. 3. j/E response applying the potential-time routine indicated in (b).

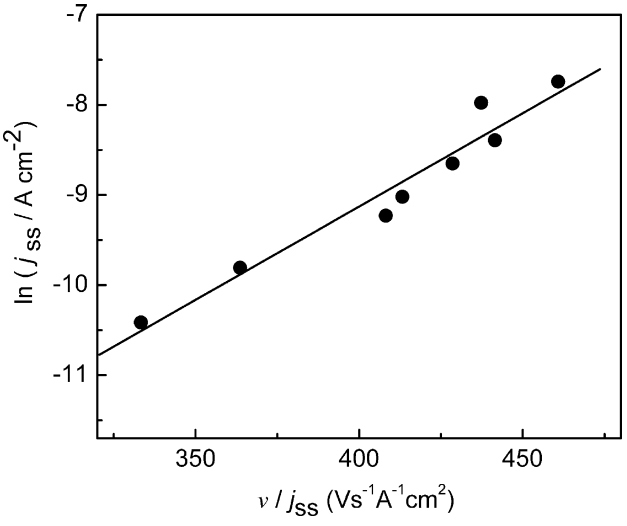

Fig. 4. Dependence of j_{ss} on v.

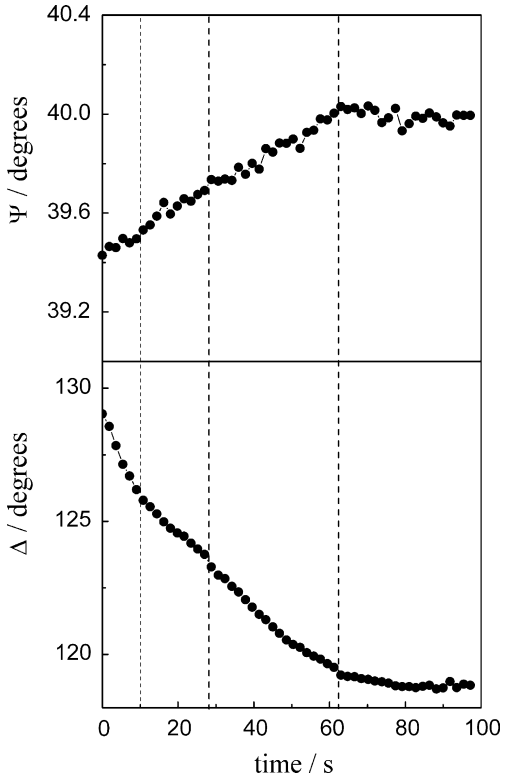

Fig. 5. Dependence of the ellipsometric angles (Ψ and Δ) on time. Positive scan: 0–60 s. Negative scan: 60 s and up.

Region 2: from *ca.* 8 s up to 28 s, which corresponds to the Sn(IV) anodic film growth from −0.2 V up to *ca.* 0.7 V.

Region 3: from *ca.* 28 s up to 60 s, corresponding to the further anodic growth of the tin oxide film at potentials exceeding 0.7 V.

Region 4: after 60 s (negative scan), where the ellipsometric angles Ψ and Δ do not exhibit any important changes due to the rapid decrease of the growth rate of the oxide film.

Fig. 6 shows the Ψ–Δ response during the potentiodynamic growth of the tin oxide film. Although the dependence of Ψ or Δ with time (Fig. 5) exhibits the different stages corresponding to the sequence of different processes taking place consecutively during the overall anodic oxide growth, no remarkable features can be seen in the Ψ–Δ relationship. This result suggests that the optical properties (refractive index, n_f, and extinction coefficient, k_f) of the film in the different potential regions during electroformation and growth, are not very different from each other. Furthermore, the slight variation of the ellipsometric angles Ψ and Δ would indicate that relatively low values of thickness are involved. The Ψ–Δ response (Fig. 6) can be reasonably fitted employing a single-layer isotropic film model [13–17]. The complex refractive index ($\tilde{n}_f = n_f - ik_f$) value obtained from the fitting procedure for the tin oxide film, results $\tilde{n}_f = 1.45 - 0.0013i$. Nevertheless, it should be taken into account that assuming a single-layer model is

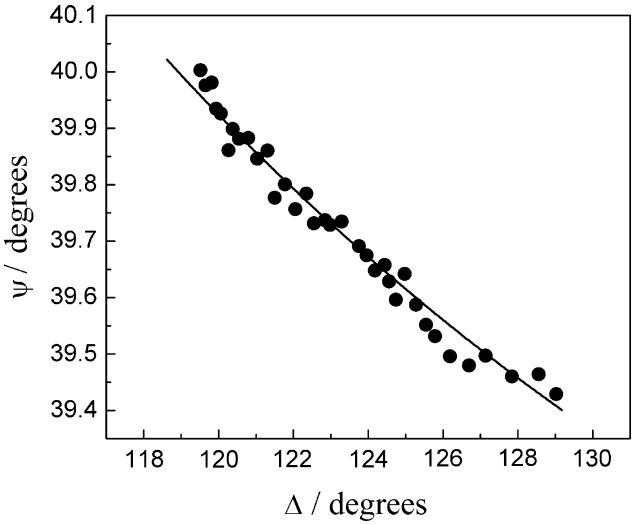

Fig. 6. Ψ–Δ plot for anodization of polycrystalline Sn at 0.050 V s^{-1} in borate solutions (pH 8.9). (●) Experimental data for film growth and (—) calculated curve for a simple isotropic layer. $n = 1.45$, $k = 0.0013$.

only approximate. In addition, the generation of some roughness on the tin surface during the first stages of metal electro-oxidation where soluble species formation takes place, would affect the optical properties obtained from modelling. The low value of refractive index obtained, $k_f = 0.0013$, indicates that the tin oxide film is practically transparent. Furthermore, the value $n_f = 1.45$ obtained, is lower than those reported for typical "valve" metals like Ta [18], Zr [19], V [20], Mo [21], W [14,15] or Bi [16], where values ranging from 2.0 to 2.3, which are similar to those of the corresponding crystalline oxides, have been informed. On the other hand, oxide layers formed on Ni [22] and Fe [23], which are considerably more hydrated and probably amorphous in nature, exhibit values of refractive index of 1.46 and 1.41, respectively. Materials nearly transparent that exhibit optical properties more similar to the electrolyte ($1.33 < n < 1.36$, in the visible region) than to the corresponding crystalline solid itself, present generally a low density and evidence a high hydration level [24]. This would indicate that the tin oxide film obtained after a potentiodynamic scan is highly hydrated. The value obtained is also lower than that reported for thin oxide layers obtained potentiostatically after a two-hour polarization [4], where is known that dehydration and ageing processes take place.

Fig. 7 shows the dependence with potential of the oxide thickness, d, obtained from the fitting procedure. In the −0.2 V to 1.8 V potential range where the tin anodic oxide growth takes place, two distinct regions with a different growing rate, are clearly seen. The electric field, $\overline{E} = E/d$, obtained from the d/E slope up to *ca.* 0.7 V is around 13 MV cm^{-1}, while the value at potentials more positive than 0.7 V results 9.8 MV cm^{-1}. This last value corresponds to the potential region where a slight increase in the steady-state current for growth is obtained (see Fig. 1), indicating a slight change in the physical properties

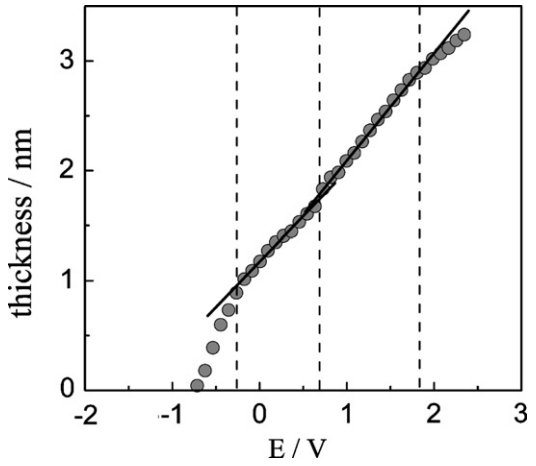

Fig. 7. Dependence of the thickness with potential. The solid lines indicate a linear fit.

of the oxide film. At potentials more positive than *ca.* 1.8 V, deviations attributed to the oxygen evolution reaction are obtained.

Although the thickness values should be taken in a judicious way due to the simplified optical analysis, it can doubtless concluded that in the −0.2 V to 1.8 potential range, tin oxide grows as a continuous film following a kinetic law corresponding to a high-field as in typical "valve" metals.

3.3. Electrical properties

In order to obtain the electrical properties of the tin oxide/hydroxide films formed on tin in alkaline borate solutions, impedance spectra of layers grown at different potentials were obtained. Films of different thickness were prepared by applying a potential scan up to a given formation potential, ($0.32\ \text{V} \leqslant E_f \leqslant 1.72\ \text{V}$) and afterwards, the impedance spectra were obtained at the open circuit potential.

Fig. 8 shows the Bode plots for the EIS spectra recorded for films formed at different potentials in the frequency range 0.1 Hz–10 kHz. The $\log|Z| - \log w$ plots (Fig. 8a) exhibit a region of constant impedance at high frequencies that is independent of the final formation potential, which is related to the solution resistance. At intermediate frequencies, the linear $\log Z - \log w$ variation characteristic of a capacitive behaviour, is attributed to the capacitance of the oxide film. At low frequencies, the response is again resistive and strongly dependent of the final formation potential of the oxide and is associated with the oxide resistance. The inset in Fig. 8a shows the intermediate frequency region in detail. As the oxide formation potential is increased the capacitive region is shifted to higher frequencies indicating a decrease of oxide film capacitance. On the other hand, oxide film resistance at low frequencies initially increases with formation potential (up to 1.12 V) but then decreases markedly as formation potential is made more positive than this value. The phase angle-frequency dependence (Fig. 8b) shows phase angle values nearly 0 at high frequencies, a capacitive behaviour at intermediate frequencies, and the phase angle decreases again reaching values near to 0 at low frequencies, as expected. The phase angle-frequency dependency clearly indicates the existence of only one capacitive contribution. The electrical response was analyzed using an equivalent electrical circuit for a single oxide layer in terns if a simple electrical R_s(RC) circuit, where R_s represents the solution resistance and R and C are associated with the oxide resistance and capacitance, respectively. The oxide film capacitance is replaced by a constant phase element (CPE) in order to take into account non-ideal capacitive behaviour of inhomogeneous oxide films [25]. Fig. 9 shows that the impedance response for films of different thickness can be adequately fitted by the inhomogeneous single layer model. These results are consistent with the behaviour obtained for other oxides formed on valve metals like hafnium [26,27] and zirconium [28].

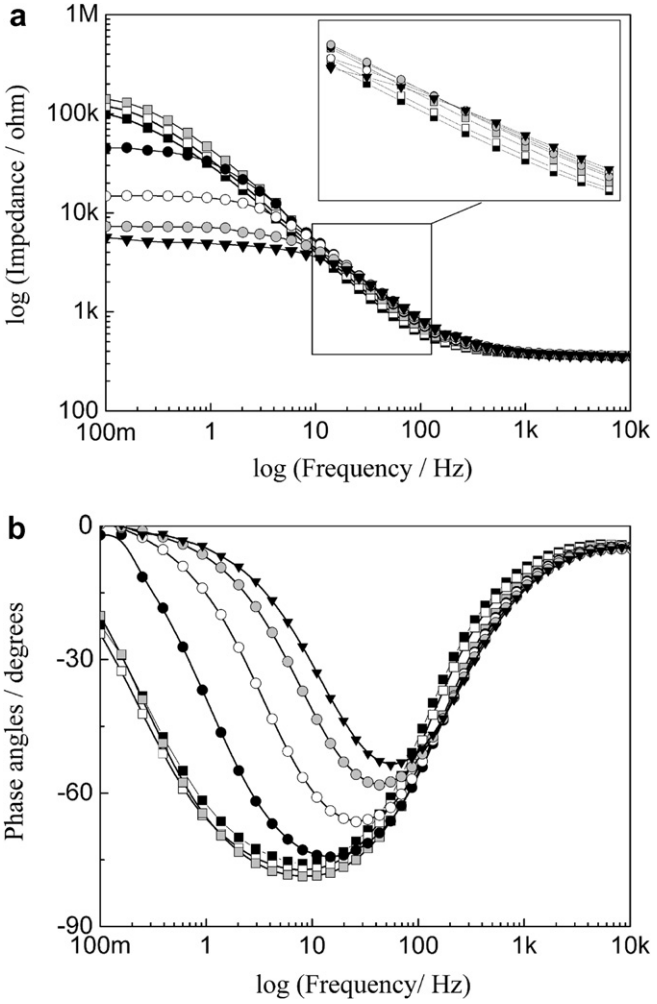

Fig. 8. Bode diagrams for films of tin oxide/hydroxide films formed up to different potential values. $Ef = 0.32$ V (■), 0.52 V (□), 1.12 V (◘), 1.32 V (●), 1.42 V (○), 1.52 V (◙), 1.72 V (▼). (a) log Z *vs.* log w. (b) Phase angle *vs.* log w.

From the fitting of the experimental data in Fig. 8 with the inhomogeneous single-layer model using the Boukamp routines [29], values of the electrical parameters R and C for the oxide films were obtained. Fig. 10 shows the dependence of R and C^{-1} on the formation potential for the oxide film. Initially, R exhibits a slight increase with potential, in good agreement with the increase of layer thickness. At approximately 1.2 V, a drastic decrease of the oxide resistance is obtained and then R values remain practically constant (Fig. 10a). In addition, the $C^{-1} - E$ plot (Fig. 10b) shows a similar trend. This behaviour is consistent with the ellipsometric data, which indicate that oxide layers grown in different potential ranges have different physical properties. Moreover, similar changes have been obtained by reflectometry [4]. From the linear $C^{-1} - E$ dependence and using the electric field value obtained from the ellipsometric thicknesses, the an estimation of 11.7 for the dielectric constant of tin oxide grown up to 1.2 V can be made assuming a roughness factor of 1.

The increase of the capacitance value at potentials more positive than 1.2 V can not be explained as a decrease of the thickness because the ellipsometric data indicate that the oxide continues growing up to 1.8–2 V. A drastic decrease of the electrical parameters R and C^{-1} has also been found during the growth of other oxides on valve metals and has been called "*anodic oxide layer rupture*" [30]. When the metal is anodized and oxide growth takes place, stress due to some phase transformations (e.g. crystallinity increase), and changes in the growth kinetics or hydration/dehydration processes of the films can be developed and therefore they can generate a partial rupture of the film if a critical thickness is reached [30]. Then, the oxide layer continues growing but as a porous or cracked layer, which would have different properties. A similar phenomenon has also been observed during oxide growth on hafnium [31].

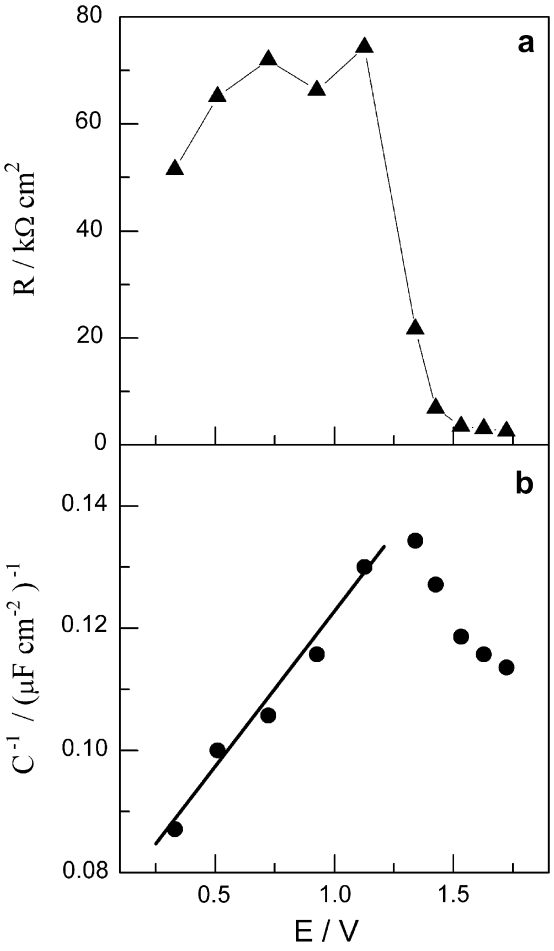

Fig. 10. (a) Dependence of R on E. (b) Dependence of C^{-1} on E.

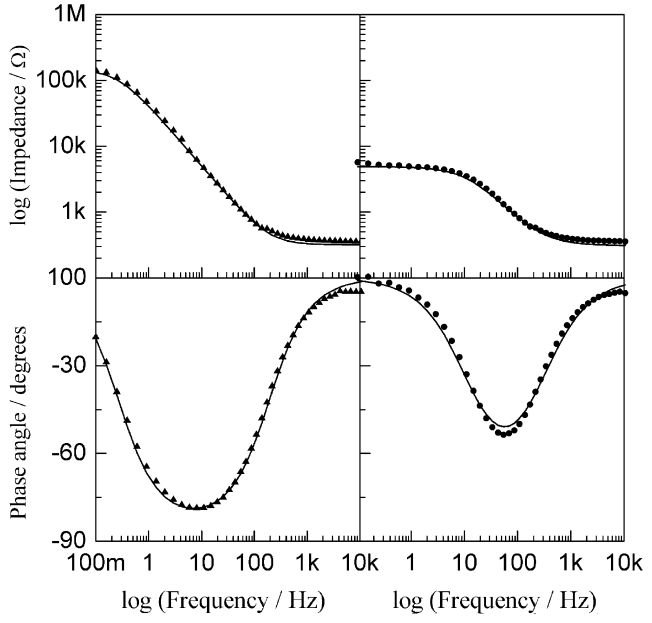

Fig. 9. Bode diagrams for films formed up to 1.12 V (▲) and 1.72 V (●); (—) fitting with the inhomogeneous single-layer model.

4. Conclusions

The kinetic characteristics of anodic growth of tin oxide films in aqueous borate solutions at potentials more positive than −0.2 V (SHE) have been obtained. After the initial formation of a hydrated oxide/hydroxide layer associated with the stepwise oxidation of Sn to Sn(IV) species under an ohmic resistance control, a continuous tin oxide film grows following an ionic-conduction mechanism under the influence of a high electric field across the film as in typical "valve" metals. From the potentiodynamic analysis, the values for the parameters A and β characterising the anodic growth were obtained. Film optical properties obtained from ellipsometric measurements, indicate that under the present conditions tin oxide films are practically transparent and highly hydrated. In addition, from the thickness-potential dependence the high-field anodic growth is corroborated and values for the electric field are obtained. Electrochemical impedance results are explained in terms of an inhomogeneous single-layer film model. Spectra show the typical response for a dielectric

material and from the capacitance/potential dependence the dielectric constant of the hydrated tin anodic oxide film can be estimated. In addition, the occurrence of an anodic oxide layer rupture at potentials more positive than *ca.* 1.2 V is apparent.

Acknowledgements

Financial support of the Consejo Nacional de Investigaciones Científicas y Técnicas of Argentina (CONICET), the Agencia Nacional de Promoción Científica y Tecnológica (ANPCYT), the Agencia Córdoba Ciencia S.E. and the Secretaría de Ciencia y Tecnología (SECYT-UNC) is gratefully acknowledged.

References

[1] V. Brunetti, M. López Teijelo, J. Electroanal. Chem. 613 (2008) 9–15.
[2] S.D. Kapusta, N. Hackerman, Electrochim. Acta 25 (1980) 949–955.
[3] S.D. Kapusta, N. Hackerman, Electrochim. Acta 25 (1980) 1001–1006.
[4] S.D. Kapusta, N. Hackerman, J. Electrochem. Soc. 129 (1982) 1886–1889.
[5] A. Ammar, S. Darwish, M.W. Khalil, S. El-Taher, Electrochim. Acta 33 (1988) 231–238.
[6] I.A. Ammar, S. Darwish, M.W. Khalil, S. El-Taher, Corrosion 46 (1990) 197–202.
[7] M. Metikos-Hukovic, A. Resetic, V. Gvozdic, Electrochim. Acta 40 (1995) 1777–1779.
[8] W.H. Press, B.P. Flannery, S.A. Teukolsky, W.T. Vettering, Numerical Recipes: The Art of Scientific Computing, Cambridge Press, Cambridge, 1986.
[9] S.T. Amaral, E.A.M. Martini, I.L. Muller, Corros. Sci. 43 (2001) 853–879.
[10] M.J. Dignam, in: J.O'M. Bockris, B.E. Conway, E. Yeager, R.E. White (Eds.), Comprehensive Treatise of Electrochemistry, vol. 4, Plenum Pub. Corp., New York, 1981, p. 247.
[11] J.W. Schultze, M.M. Lohrengel, Electrochim. Acta 45 (2000) 2499.
[12] E.M. Patrito, R.M. Torresi, E.P.M. Leiva, V.A. Macagno, J. Electrochem. Soc. 137 (1990) 524–530.
[13] R.M.A. Azzam, N.M. Bashara, Ellipsometry and Polarized Light, Elsevier Science Publishers, 1977–1987.
[14] M.A. Perez, M. Lopez Teijelo, Thin Solid Films 449 (2002) 138–146.
[15] M.A. Perez, M. Lopez Teijelo, J. Phys. Chem. B 109 (2005) 19369–19376.
[16] M.A. Perez, M. Lopez Teijelo, J. Electroanal. Chem. 583 (2005) 212–220.
[17] M.A. Perez, O.E. Linarez Perez, M. Lopez Teijelo, J. Electroanal. Chem. 596 (2006) 149–156.
[18] J.L. Ord, P. Wang, J. Electrochem. Soc. 130 (1983) 1809.
[19] E.M. Patrito, V.A. Macagno, Electrochem. Soc. 140 (1993) 1576.
[20] J.C. Clayton, D.J. De Smet, Electrochem. Soc. 123 (1976) 174.
[21] D.J. De Smet, J.L. Ord, Electrochem. Soc. 130 (1983) 280.
[22] M.A. Hopper, J.L. Ord, Electrochem. Soc. 120 (1973) 183.
[23] Z.Q. Huang, J.L. Ord, Electrochem. Soc. 132 (1985) 24.
[24] S. Gottesfeld, in: A.J. Bard (Ed.), Electroanalytical Chemistry, a series of advances, Marcel Decker, New York, 1989.
[25] J. Ross Macdonald, Impedance Spectroscopy: Emphasizing Solid Materials and Systems, John Wiley & Sons, 1987.
[26] M.J. Esplandiu, E.M. Patrito, V.A. Macagno, J. Electroanal. Chem. 553 (1993) 161–176.
[27] M.J. Esplandiu, E.M. Patrito, V.A. Macagno, Electrochim. Acta 40 (1995) 809–815.
[28] E.M. Patrito, V.A. Macagno, J. Electroanal. Chem. 375 (1994) 203–211.
[29] B.A. Boukamp, Equivalent Circuit: Users' Manual, University of Twente, A.E. Enschede, The Netherlands, 1989.
[30] J.M. Albella, J. Montero, J.M. Martinez-Duart, J. Electrochem. Soc. 131 (1984) 1101–1104.
[31] M.J. Esplandiú, Ph.D. Thesis, National University of Córdoba, Argentina, 1995.